FINAL TECHNICAL REPORT

HAYWARD, CALAVERAS, AND MISSION FAULT SUBSURFACE SLIP FROM JOINT ANALYSIS OF MICROEARTHQUAKE RECURRENCE AND SPACE GEODESY

National Earthquake Hazard Reduction Program

U.S. Geological Survey

NEHRP Program Element: I, Products for Earthquake Loss Reduction

Award Number: 02HQGR0062

Principal Investigator:

Roland Bürgmann (University of California, Berkeley)

Department of Earth and Planetary Science
307 McCone Hall
Berkeley, CA 94720
Phone: (510) 643-9545
FAX: (510) 643-9980
e-mail: burgmann@seismo.berkeley.edu

Research supported by the U.S. Geological Survey (USGS), Department of the Interior, under USGS award number 02HQGR0062. The views and conclusions contained in this document are those of the authors and should not be interpreted as necessarily representing the official policies, either expressed or implied, of the U.S. Government.

HAYWARD, CALAVERAS, AND MISSION FAULT SUBSURFACE SLIP FROM JOINT ANALYSIS OF MICROEARTHQUAKE RECURRENCE AND SPACE GEODESY

Award Number: 02HQGR0062

Roland Bürgmann, University of California, Berkeley

Department of Earth and Planetary Science
307 McCone Hall
Berkeley, CA 94720-4767
Telephone: (510) 643-9545; FAX (510) 643-9980; burgmann@seismo.berkeley.edu

Technical Abstract

The Hayward and Calaveras faults relieve strain in large earthquakes, but also by steady slip known as aseismic creep. We combine surveys of crustal deformation using space based geodetic techniques such as GPS and InSAR with traditional survey techniques to quantify surface deformation from locked and creeping faults. We solve for the slip-rate distribution on the Hayward fault by performing a least-squares inversion of geodetic and seismic data sets. InSAR data from many independent ERS interferograms are stacked to obtain range-change rates from 1992 to 2000. Horizontal surface displacement rates at 141 benchmarks are measured using GPS from 1991 to 2002. Surface creep observations and estimates of deep slip rates determined from characteristic repeating earthquake sequences are also incorporated in the inversion. The densely spaced InSAR data require a non-planar fault surface to adequately model the near-fault data. The fault is discretized into 283 triangular dislocation elements that approximate the non-planar attributes of the fault surface. The inferred slip-rate distribution is consistent with a fault that creeps aseismically at a rate of 5 mm/yr to a depth of 4 to 6 km. The InSAR data require an aseismic slip-rate that approaches the geologic slip-rate on the fault beneath San Pablo Bay while a low slip-rate patch of less than 1 mm/yr is inferred beneath San Leandro. We calculate that the entire fault is accumulating strain at the rate of a M 6.8 per century. However, this estimate of moment release represents upper bound for any coseismic event because we do not know how much of the strain will be released through aseismic processes such as afterslip.

Non Technical Abstract

The earthquake cycle involves the accumulation of strain along locked faults followed by the catastrophic release of strain during an earthquake. The Hayward and Calaveras faults relieve strain in large earthquakes, but also by steady slip known as aseismic creep. The fundamental questions we investigate are where and how fast is strain being released by creep? We combine surveys of crustal deformation using space based geodetic techniques such as GPS and InSAR with traditional survey techniques to quantify surface deformation from locked and creeping faults. Using additional information from characteristically repeating microearthquakes and computer models, we determine the distribution and rate of creep at depth on the East Bay faults. These detailed maps of locked and creeping fault patches improve our estimates of seismic potential and hazard along major faults in the San Francisco Bay area.

HAYWARD, CALAVERAS, AND MISSION FAULT SUBSURFACE SLIP FROM JOINT ANALYSIS OF MICROEARTHQUAKE RECURRENCE AND SPACE GEODESY

Award Number: 02HQGR0062

Table of Contents

Section *Page*

HAYWARD, CALAVERAS, AND MISSION FAULT SUBSURFACE SLIP FROM JOINT ANALYSIS OF MICROEARTHQUAKE RECURRENCE AND SPACE GEODESY

1. INTRODUCTION

The San Francisco Bay area (“Bay Area”) is home to about 5.9 million residents and is an important economic center. Additionally, the “Silicon Valley,” located in the southern Bay Area, is host to a considerable portion of the high-technology industry. It is evident that large earthquakes in this area have the potential to cause significant loss of life and property damage. The eastern Bay Area has experienced numerous historical earthquakes, including several moderate to large magnitude events on the Calaveras and Hayward faults. Adequate earthquake preparedness is critical, and it is necessary that the seismic hazard of the region be adequately investigated so the potential hazards are identified. By identifying and evaluating the active deformation occurring along the East Bay fault zones, we can identify potential hazards and thus assist the development of earthquake policy.

1.1 Project Components

The primary objective of this study is to monitor the spatially and temporally complex active deformation field in the eastern Bay Area along the Hayward, Mission and Calaveras fault zones. Information from this study allows for the evaluation of the fault slip rates, which can be used to evaluate earthquake hazards in the region. This project addresses the seismic potential and natural hazard presented by the East Bay faults to the San Francisco Bay area through the use of space-based technology, namely GPS and differential radar interferometry (InSAR), combined with high-resolution observations of microearthquake activity on the faults. This research provides detailed information on the magnitude of subsurface aseismic fault slip and it's variation in space and time. This project directly contributes to reducing losses from earthquakes in the San Francisco Bay area by contributing reliable estimates of earthquake potential (size and slip-deficit accumulation rates of locked fault segments) along three major fault segments.

Imaging distributed slip on subsurface faults from surface displacements is a difficult task, plagued by limits in the spatial resolution of the surface displacements and ambiguities in the depth resolution of slip variations. The ability to derive even just a few point measurements of fault slip at depth adds invaluable constraints on the spatial distribution and magnitude of aseismic slip along fault surfaces. Therefore, inversions aided by such constraints can significantly sharpen the resolution of locked patches along the Hayward (HF), Calaveras (CF) and Mission (MF) faults. Subsurface slip-rate estimates can be integrated with surface and space based geodetic measurements in inversions in a straightforward manner. We have successfully applied joint geodetic and repeating earthquake techniques to the northern HF using INSAR, GPS, creep and NCSN archival data).

The aseismic slip-rate distribution at depth on the Hayward fault is calculated through the use of space-based technology, namely GPS and differential radar interferometry (InSAR), and fault creep rates (Schmidt, 2002; Schmidt and Bürgmann, 2002). Surface creep rates and point creep rates at depth determined from characteristic repeating microearthquake sequences are used as additional constraints in the geodetic inversion. The ability to derive point measurements of fault slip at depth can significantly sharpen the resolution of the spatial distribution and magnitude of aseismic slip along fault surfaces. Using a double-difference earthquake relocation program, we can resolve the seismic structure of the Hayward fault in greater detail, which provides important information about sub-surface fault geometry and the relative location of point slip rates with respect to each other along the fault plane. Our results provide detailed information on the magnitude of subsurface aseismic fault slip and its variation in space and time.

2. OBSERVATIONS AND ANALYSIS

This project includes the continued analysis and interpretation of past GPS results, as well as the enhancement of the vigorous geodetic monitoring effort in the eastern Bay Area. The GPS measurements directly constrain the slip rates of major faults. Additionally, dense geodetic networks were used to estimate the locking depth along faults and estimate the amount of fault slip accommodated by aseismic creep. We believe that highest-quality geodetic data of the complex southern Bay Area velocity field, together with rigorous models of the observed deformation, provide important constraints on the nature of fault loading and fault interaction. These results are crucial for better estimates of earthquake hazard in the Bay Area. Densely spaced networks observed in yearly campaigns together with a larger network of continuously operating BARD stations provide the optimal configuration to achieve these goals. Because of its unsurpassed spatial resolution, we have made significant advances in integrating InSAR measurements of crustal deformation in the Bay area (Bürgmann et al., 2000). Finally, our studies of aseismic fault slip along the Hayward, Calaveras and San Andreas fault now benefit from additional constraints provided by repeat intervals of identical microseismic events (Nadeau and McEvilly, 2000, Bürgmann et al., 2000).

2.1 GPS Data Collection and Analysis

Data collection methods included the use of BARD network continuous GPS stations and periodic campaign-style GPS network observations. Observations were coordinated with the USGS surveying of the southern Bay Area profile networks. Yearly observations have allowed us to monitor the continuing development of deformation and improve the precision of geodetic measurements. In addition to continuity of data, yearly observations also provide greater efficiency in project logistics (i.e., landowner contact, site access changes, etc.).

As part of our ongoing effort to monitor active deformation along the Hayward fault, we determine positions of over fifty benchmarks within ten kilometers of the fault (Figure 1). These measurements will provide an unprecedented spatial resolution of GPS measurements about an active fault. The first surveys of most benchmarks were made in 1998, and our group has been returning each summer to take new measurements. The data from these campaigns are currently being integrated with other regional data, including existing continuous stations and ongoing campaigns active on the Calaveras and San Andreas faults. Combined, these data sets provide a complete picture of the regional surface deformation, strain partitioning between the faults, and interseismic strain accumulation. We collected GPS measurements from 41 benchmarks in the vicinity of the Hayward fault, most in urban settings that require an operator to be with the station during the entire period of data collection (lasting at least 8 hours). Many stations have been occupied more than once, resulting in over 100 days of total data collection. In order to better integrate our campaign solutions with other data sets, we are currently reprocessing our entire data holdings and computing loosely constrained solutions in GAMIT. Preliminary results show excellent agreement with our previous processing and with other existing data sets. For example, a comparison of surface creep rates measured using GPS during this project and triangulation work by Lienkaemper and Galehouse (1997) show similar results (Figure 2), especially for stations where the most recent data has been successfully processed.

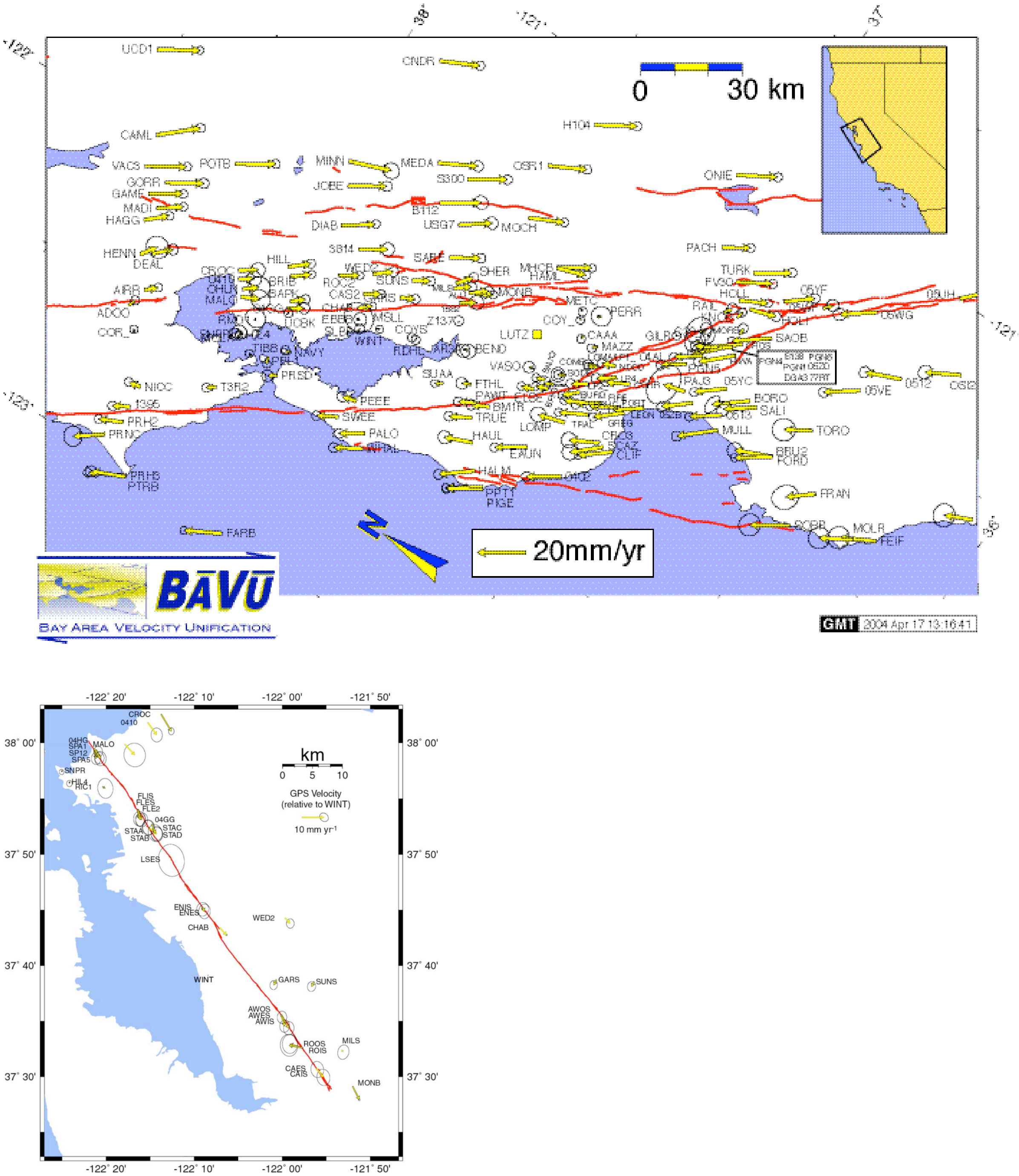

Figure 1. (Top) Compilation of continuous and campaign GPS station velocity field spanning 1994-2002 in oblique Mercator projection about the pole of Pacific-plate-to-SNGV block rotation. Data are from UCB and USGS campaign measurements and the BARD continuous network and are the first version of the combined velocity map (BAVU 1.0) from consistently reprocessed GAMIT solutions shown relative to station LUTZ in San Jose. The displacement field widens north of Monterey Bay as slip is being transferred from the central San Andreas fault to the Calaveras-Hayward and other East Bay faults. (Bottom) Close-up map of GPS velocities along the Hayward fault.

2.2 InSAR Analysis of Interseismic Deformation

Geodetic measurements of surface displacements surrounding a fault can be used to determine subsurface slip rates on dislocations in an elastic half-space model. If fault slip occurs at relatively shallow depth, as is the case for faults experiencing creep in the upper 10 km of the crust, such measurements have to be closely spaced near the fault. However, precisely surveyed GPS sites in the San Francisco Bay area are generally spaced more than 10 km apart and it is therefore difficult to determine a reliable slip estimate from existing point measurements alone. Space based interferometric synthetic aperture radar (InSAR) can map ground deformation at 10s-of-meter spatial resolution with sub-cm precision (Bürgmann et al., 2000a, b). InSAR only provides measurements of one component of the displacement field along the look direction of the radar. Thus, to improve constraints on the rate and extent of aseismic fault slip, we integrate surface creep rates established over several decades, GPS measurements of site velocities, and InSAR measured range changes. We also consider subsurface creep rates estimated from identical repeating micro-earthquakes as discussed in the following section of this report.

We use synthetic aperture radar (SAR) data collected by the European Space Agency's ERS spacecraft since 1992 to produce high-resolution surface deformation maps of range change to the spacecraft. We use InSAR data analysis techniques developed at the Jet Propulsion Laboratory. Surface displacement rates are computed from the interferograms by unwrapping angular phase delays and converting the phase delay into line-of-sight range change rates. The ERS descending orbit track trends 193.9° with the radar looking westward at a 23° off-vertical look angle. Surface displacements and resulting range change are related as $\Delta\rho = \Delta\vec{d} \cdot \vec{e}$, where $\Delta\rho$ and $\Delta\vec{d}$ are the range change and surface displacement vectors, respectively, and $\vec{e}$ is the unit vector in the range direction (Bürgmann et al., 2000). Topographic contributions to the apparent range changes are removed using a 30-m-resolution U.S. Geological Survey digital elevation model. We remove a linear displacement gradient across the SAF system, which is well constrained by the GPS velocities, from the InSAR range change data before flattening (removal of orbital ramp during processing). This interseismic deformation ramp is added back into the interferogram during the final processing steps.

In the past year, we have begun the unprecedented formal integration of now almost 200 interferograms from 3 frames covering the central Bay area (Schmidt and Bürgmann, 2003). In this approach, data from all the interferograms are formally combined in a least-squares inversion to determine a time series of range change at each image element. This analysis can resolve transient deformation episodes, such as a large 1996 slip event on the southern Hayward fault (Schmidt et al., 2002).

The utility of InSAR depends on surface properties being coherent between the pair of scenes used to form the interferogram. Any change in surface properties due to vegetation, erosion, or land use will impact the quality of the InSAR measurement (Bürgmann et al., 2000). Densely vegetated areas and rough topography away from mostly developed areas limit the region of adequate correlation. Thus we find that while conditions in the urban Bay area along the Hayward fault are suitable for InSAR (Bürgmann et al., 1998, 2000), it is more difficult to acquire useful data along much of the Calaveras and San Andreas faults. We thus put a lot of effort into utilizing InSAR over areas with relatively scattered “islands of coherence”. We are using both improved phase unwrapping algorithms and permanent scatterer techniques to allow for the inclusion of data in these regions (Johansen and Bürgmann, 2001, 2002). This approach relies on methods to identify individual coherent pixels (such as buildings or outcrops) in an otherwise incoherent region. Figure 2 shows a stack of 8 1992-2000 interferograms, with gray shaded zones indicating incoherent regions, where vegetation or erosion doesn’t allow for interferometry. The Hayward fault is clearly visible as a step in the otherwise smoothly varying range-change field. This stacked data set is used in the inversion for aseismic fault slip rates on the Hayward fault, described below.

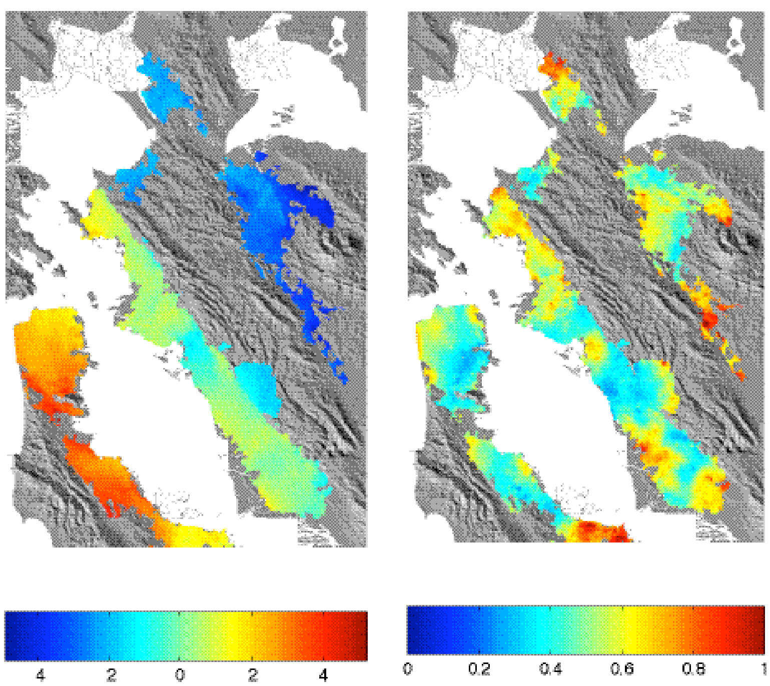

Figure 2. To the left, a stack of 8 differential interferograms of the San Francisco Bay Area shows the range change rate (in mm/yr) over a 7.5-year period. Superimposed over a shaded relief image is the change in range along the look direction of the satellite. Surface creep on the Hayward fault is represented by a discontinous jump in phase observed in Pinole, Castro Valley, and Fremont. The Interseismic strain profile across the Bay Area related to distributed elastic deformation across the plate boundary is represented by the gradient from red to blue. The right panel shows the 1-sigma error estimate of the range-change rates determined from the data scatter (in mm/yr).

2.3 East Bay Faults Point Slip Rate Measurements From Earthquake Recurrence

Following the successful comparison of repeating earthquake data with geodetic measurements at Parkfield (Nadeau and McEvilly, 1998) and along the northern Hayward fault (Bürgmann et al., 2000), we are now working on integrating geodetic and seismic data in a similarly complementary way along the whole East Bay fault system. We have completed our initial and computationally intensive search for characteristic sequences on the southern Hayward, Calaveras and Mission faults. Our search for repeaters revealed large numbers of highly similar and repeating events (coherency > 0.95) in the NCSN catalog distributed widely on all three faults. Using NCSN surface data the fractions of identifiable repeaters is about 10%, 15% and 25%, for the northern Hayward fault, southern Hayward/Mission fault and Calaveras fault segments respectively. The lower fractions are explainable in part by lower slip rates and higher magnitude thresholds, since under these conditions recurrence intervals may be longer than observation times. In our prototype analysis on the northern Hayward fault, we showed that sufficient information was available to resolve spatially varying features of slip using surface NCSN data but that monitoring of short-term temporal variations was not practical with the limited resolution of the surface data on such a slowly moving fault. To the southeast, on the faster moving Mission and Calaveras faults, we have found sufficient rates of quake repetition to allow us to use NCSN data for monitoring transients (Figure 3) as is currently being achieved on the faster slipping San Andreas fault to the West (Nadeau and McEvilly, 1999). Using NCSN arrival times, we have relocated seismicity using a double-difference earthquake relocation program (Figure 3) and are evaluating the more highly resolved spatial and temporal seismicity patterns in relation to surface and spaced based deformation estimates, to the spatial and temporal distribution of repeating earthquake sequences and to the post-seismic period following the 1984 Morgan Hill earthquake.

Our preliminary findings indicate that, as at Parkfield and on the creeping section of the San Andreas fault, the locations of repeating earthquake sequences are confined to the central portion of seismicity within large fault zones. However, repeating earthquakes are not ubiquitous on all faults. Our search for characteristic quakes failed to identify any repeating sequences on the Calaveras fault just north of its juncture (Manaker et al., 2003) with the Mission fault trend between Fremont and San Jose (Figure 3A). Furthermore, along the Mission and southern Hayward fault, repeating sequences only appear in the shallow portion of the seismogenic zone (Figure 3A, depth section). On these segments, below about 5-6 km, characteristically repeating sequences are absent while background seismicity can clearly be seen. This suggests that the boundary separating the repeating and non-repeating regions often delineates the boundary between creeping and non-creeping (locked) fault behavior at depth.

Also of note in this regard is the lack of repeating earthquake activity on two splays of transient earthquake activity emanating from the Calaveras fault south of San Jose. High precision relocations show that these splays were active during the post-seismic period following the Morgan Hill (MH) earthquake of 1984, but in subsequent years these splays have become aseismic (Figure 3, map view, 84-92.5 and 92.5 to 2002). It is not yet clear if the lack of repeating sequences on these splays is due to a relatively minor amount of slip release on the faults after MH or to a fundamental instability in the strength properties of earthquake patches on these subsidiary faults.

On the Calaveras fault during the period 1984-1992.5 repeat rates (and inferred slip rates at depth) are very high in comparison to repeat rates for sequences from 1992.5 to 2002 (Figure 3A). The NW sub-segment identified in Fig. 3A is ~11 km long and at its southeast end is ~6 km away from the epicenter of MH. The MH event ruptured to the southeast of its epicenter, and there is no indication of accelerated deep creep in the NW subsegment. However, in the year prior to the LP quake, a significant acceleration in deep creep is observed. The SE sub-segment is ~6 km long and is adjacent to the MH epicenter. There is a strong acceleration in deep creep associated with MH on this segment, particularly in the first year following the event. The rate of creep decays approximately exponentially and by early 1996 has dropped to ~0. There is no evidence of slip acceleration prior to LP on this segment. On the sub-segment further to the southeast in Figure 3 (time series not shown) acceleration following MH is even stronger, and as of early 2001 deep creep rates show continued exponential decay. We are now investigating the spatio-temporal details of the response of the Calaveras fault to the 1984 Morgan Hill and 1989 Loma Prieta earthquakes.

2.4 Numerical Mechanical Models and Data Inversion

We model the measured displacement field with rectangular displacement discontinuities for uniform slip in a homogeneous elastic half-space, or in an elastic layer above a viscous substrate. For the elastic models we calculated the elastic fields (displacements, stresses, strains, and tilts) caused by any amount of strike-slip, dip-slip, and opening displacement discontinuity on any number of arbitrarily striking and dipping rectangular fault elements. Given sufficient spatial coverage we can also resolve the spatial distribution of fault slip-rate (e.g., Harris and Segall, 1987; Du et al., 1992; Pollitz, Bürgmann, and Segall, 1998). We are particularly interested in resolving the magnitude of slip on individual faults, and the distribution of locking depth, and locked and creeping segments, along a fault. The model results, derived from the geodetic data, will provide better constraints about the potential earthquake magnitude and repeat times of a fault segment.

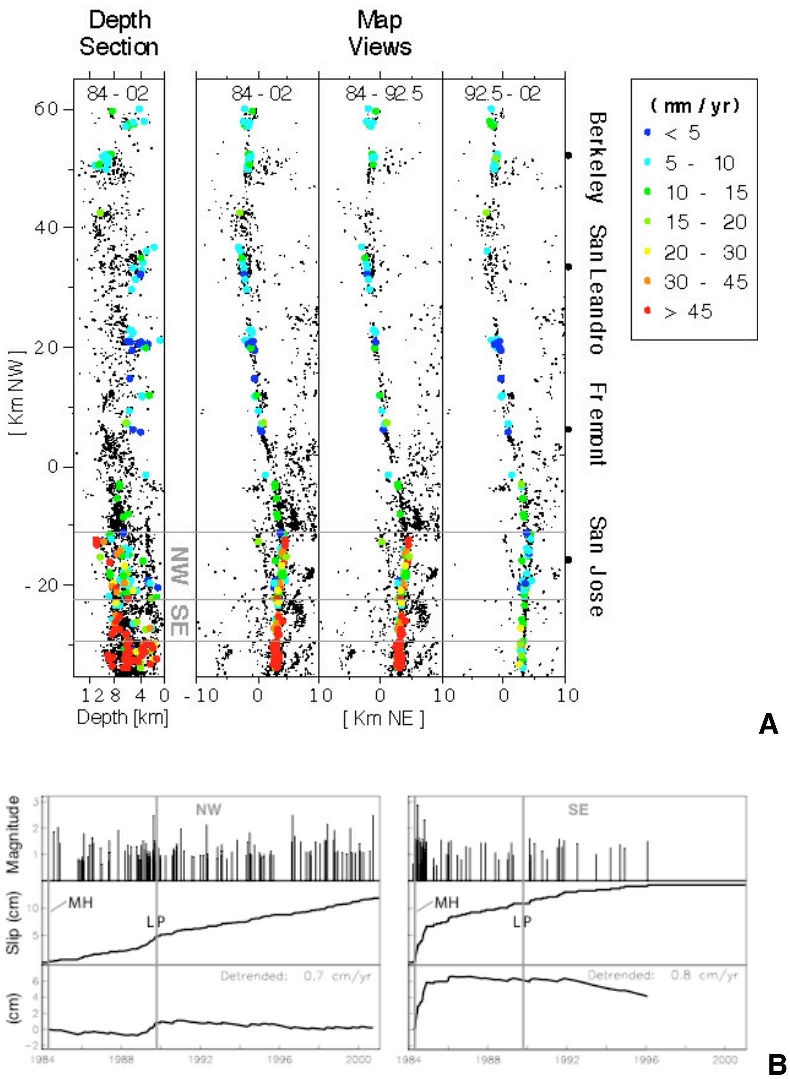

Figure 3. (A) Point fault slip rate estimates at depth inferred from recurrence intervals of characteristic micro-earthquakes, shown with the Hypo-DD relocated seismicity along a 120-km-long stretch of the East Bay area faults. Rates of slip in mm/yr are coded by color as indicated. Each color point represents the average slip rate between time sequential pairs of characteristic events in a sequence. Left panel shows, in depth section, all slip rate pair estimates and background seismicity for the time period 1984-2002. The remaining panels show in map view data for 1984-2002, 1984 to 1992.5, and 1992.5 to 2002.2. **(B)** Time series of magnitudes (top), cumulative deep slip (middle) and detrended cumulative slip (bottom) from characteristic microearthquakes occurring on the NW and SE sub-segments shown in (A). Vertical gray lines correspond to times of the Loma Prieta (LP) and Morgan Hill (MH) earthquakes.

3. ASEISMIC SLIP ON EAST BAY AREA FAULTS

3.1 Aseismic Slip Distribution Along the Hayward Fault.

The aseismic slip-rate distribution at depth on the Hayward fault is calculated through the use of space-based technology, namely GPS and differential radar interferometry (InSAR), and fault creep rates (Schmidt, 2002; Schmidt and Bürgmann, 2002). Surface creep rates and point creep rates at depth determined from characteristic repeating microearthquake sequences are used as additional constraints in the geodetic inversion. The ability to derive point measurements of fault slip at depth can significantly sharpen the resolution of the spatial distribution and magnitude of aseismic slip along fault surfaces. Using a double-difference earthquake relocation program, we can resolve the seismic structure of the Hayward fault in greater detail, which provides important information about sub-surface fault geometry and the relative location of point slip rates with respect to each other along the fault plane. Our results provide detailed information on the magnitude of subsurface aseismic fault slip and its variation in space and time.

The Hayward fault is modeled as sub-vertical dislocations in an elastic half-space using the boundary element code POLY3D developed at Stanford University. The formulation for an angular dislocation allows for a more complex geometry than the commonly used rectangular dislocation (Okada, 1985). Surface creep rates and creep rates determined from characteristic repeating microearthquake sequences are used as additional constraints in the inversion. The deformation rate is assumed to be constant over the time spanned by the various data sets since no significant fault transients are known to have occurred on the northern and central Hayward fault during the time period of interest. Only the southern most few kilometers of the Hayward fault (km 63-68) exhibit transient behavior, which appears to be related to the stress perturbation and recovery imposed by the 1989 Loma Prieta earthquake (Lienkaemper et al., 1997; Lienkaemper et al., 2001). A weighted inversion is performed using a bounded variable least squares (BVLS) approach, which minimizes the L2 norm. Given the diversity in data used in this analysis, it is also useful to apply a factor that weights the data sets relative to one another. A smoothing constraint is imposed using the Laplacian smoothing operator. The Hayward fault is represented by an 80-km-long by 12-km-deep fault plane discretized into 283 triangular subfaults with an average dimension of 3 km (Figure 4). The Hayward fault is meshed in this way in order to accommodate the divergence of the microseismicity at depth from the mapped surface trace as well as to incorporate subsurface salients, which may affect the near-fault data.

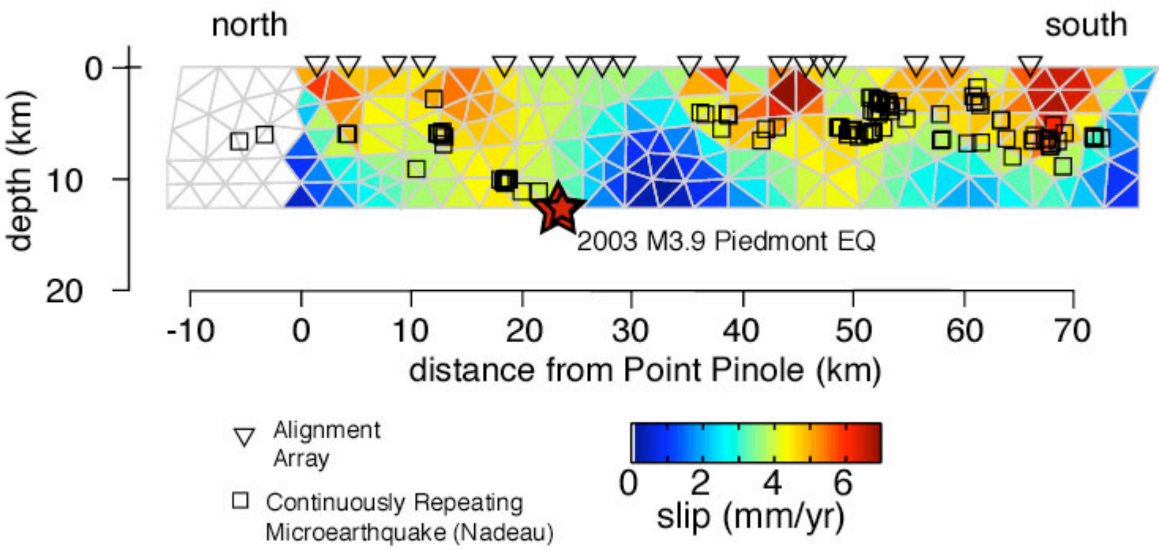

Figure 4. Top. Distribution of aseismic slip rates in mm/yr along the Hayward fault determined from GPS, InSAR, surface creep, and subsurface micro-earthquake repeater data (Schmidt, 2002).

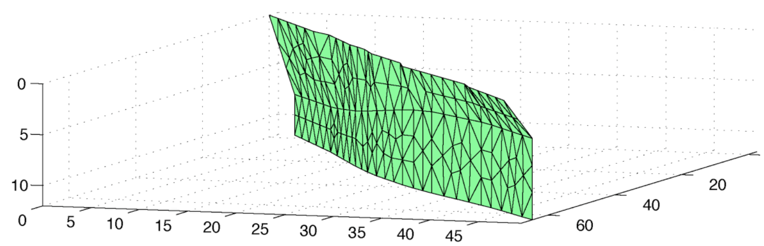

Right. 3D geometry of the boundary element mesh of triangular elements used to represent the dipping geometry of the Hayward fault.

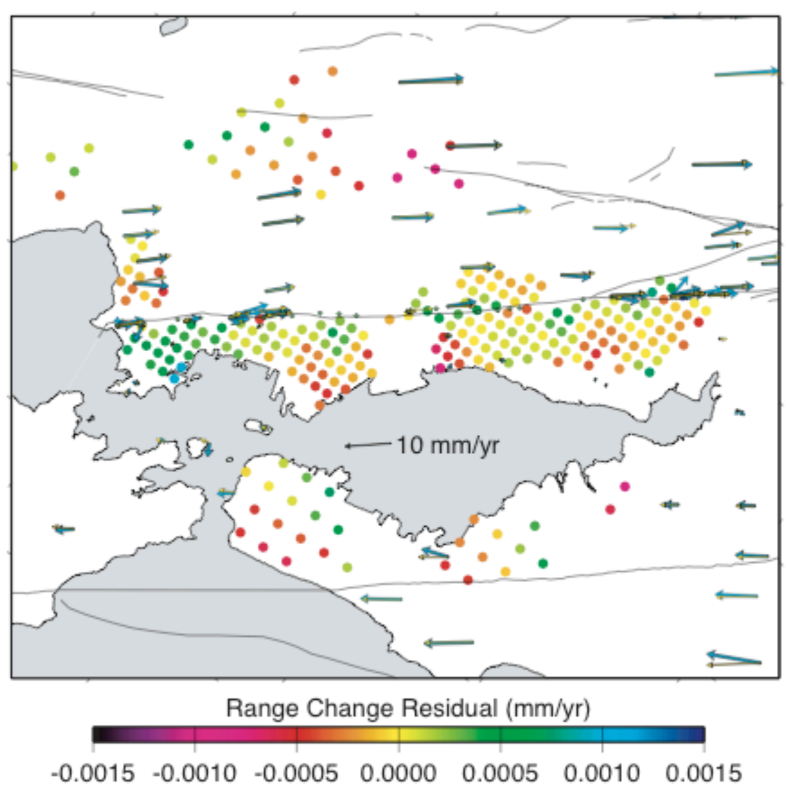

Bottom. Residual GPS-derived velocities (arrows) and InSAR-measured range change rates (color circles). The model includes regional deformation from deep dislocation below the San Andreas, Hayward, Calaveras and Greenville-Green Valley faults, and the distributed slip model from the joint inversion.

Additional model parameters include four deep, vertical dislocations located beneath the San Andreas, Hayward, Calaveras, and Greenville faults. The deep dislocations accommodate the regional strain gradient across the plate boundary. The BVLS approach allows for the right-lateral slip rate to be bound within a range consistent with geologic estimates. Subfaults on the Hayward fault are bound between 0 and 12 mm/yr, which incorporates the inferred geologic rate of 9 mm/yr plus 3 mm/yr of error (Lienkaemper et al., 1991). Each deep dislocation is bound between 0 and 30 mm/yr. Preliminary results suggest that the distribution of aseismic slip-rate on the Hayward fault indicates spatially variable fault behavior mostly consistent with the findings of previous studies (Figure 4) (Lienkaemper et al., 1991; Simpson et al., 2001). Slip-rates <1 mm/yr likely represents regions where the fault is not slipping either because the fault is locked or because slip is restrained. Locked sections may represent the nucleation site or the rupture area of future large earthquakes. The <1 mm/yr region below Oakland and at depth on the southern Hayward fault (km 20-35) agree with findings by Simpson et al. (2001) and Waldhauser and Ellsworth (2002, asperities B and C in their Figure 10).

3.2 Distribution of Interseismic Slip Rates on the Calaveras Fault

The predominant mechanism for slip transfer from the SAF to the eastern Bay Area is the Calaveras fault. It has a history of moderate earthquakes and, with the Hayward fault, presents probably the greatest seismic hazard in the southern Bay Area aside from the SAF. Understanding the processes of slip transfer in the SAF zone is important to the evaluation of the seismic hazard from secondary and tertiary active structures, including the Calaveras fault and its subsidiary structures.

The Calaveras fault is a major component of the San Andreas fault system in the San Francisco Bay area, having generated 13 earthquakes of M>5 since 1850. Where M>5 earthquakes occur along the fault, pre-mainshock and post-mainshock microseismicity is not observed in the region of coseismic slip. These aseismic areas are believed to represent locked patches of the fault that are accumulating strain to be released in M>5 events. In a recently submitted manuscript (Manaker et al., 2001, Distribution of Interseismic Slip Rates and the Potential for Significant Earthquakes on the Calaveras Fault, Central California, submitted to J. Geophys. Res.), we analyze geodetic data to better characterize the spatial distribution of interseismic slip rates on the Calaveras fault. We model the slip distribution in the seismogenic zone by inversion of over 25 years of surface deformation data, using a regional fault model with segments of the Calaveras fault discretized into ~6 km x 3 km elements, using a weighted least-squares approach with smoothing and positivity constraints.

Our discretized fault slip model consistently identifies regions of slip deficit in the seismogenic zone of the Calaveras fault that generally correspond to regions of decreased microseismicity and ruptures of previous moderate earthquakes. In particular, we find correspondence with the1979 Coyote Lake and 1984 Morgan Hill events, as well as regions where historical earthquakes on the Coyote and the Sunol-San Ramon segments have occurred. Moment magnitude calculations based on the estimated slip deficit and recurrence intervals agree with measured magnitudes of modern events and interpreted historical magnitudes. The results suggest that combining geodetically derived fault slip models with microseismicity distribution can identify specific fault regions that may pose a seismic hazard.

The Calaveras fault originates as a splay from the SAF south of Hollister and extends on a more northerly trend. The 131 km long fault is a complex system with a creeping southern segment that extends from its origin near the San Andreas fault south of Hollister its complex splaying with the Hayward and Mission faults near Fremont (Rodgers and Halliday, 1992). North of this point is a largely aseismic segment that exhibits little creep or is locked (Oppenheimer and Lindh, 1992). The northern segment continues to the Walnut Creek-Danville area where it is believed to splay into an extensional right stepover to the Concord fault (Smith, 1992).

The Calaveras fault has produced several moderate earthquakes in the last 160 years. These include a recent series of three north propagating sequential earthquakes along the northern part of the creeping southern segment (Figure 5, M 5.9 on 6 August 1979, M6.2 on 24 April 1984, and M5.1 on 13 June 1988) (Du and Aydin, 1993), as well as historical records of an estimated M6.4 earthquake on 3 July 1861 (Rodgers and Halliday, 1992), and recent earthquakes swarms in 1970 and 1990 with maximum magnitudes in the M4.0-4.5 range on the northern segment (Simpson, et al, 1992).

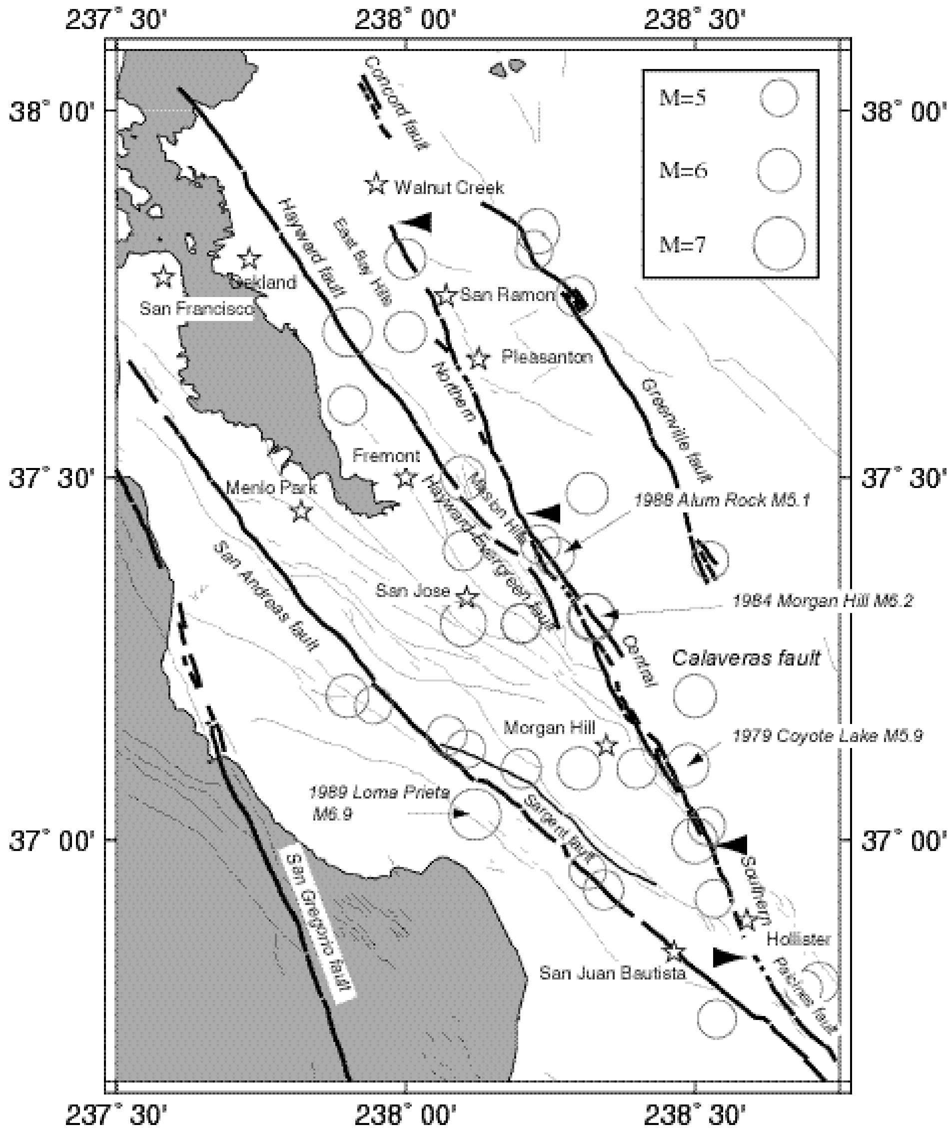

Figure 5. Regional fault map of southern Bay area with historical earthquakes. Scaled circles show historical seismicity from 1858 to 1998 of magnitude ≥ 5.

Extensive geodetic monitoring of the Calaveras fault was conducted in the 1970's and 80's by the U. S. Geologiocal Survey (Savage, et al., 1979; Prescott et al., 1981; Prescott and Lisowski, 1983). These data provided a foundation for the study of strain partitioning to the east of the SAF in the eastern and southern Bay Area. Rates of strike-slip and contraction deformation prior to the 1989 Loma Prieta temblor were evaluated. We have surveyed a combination of small (1-5 km) and medium (5-40 km) geodetic networks across the Calaveras fault with GPS to measure the surface displacement field associated with the fault. The sites surveyed included portions of USGS Hollister network, Grant network, Calaveras network, Veras network, Black Mountain Profile network and California Department of Transportation High Precision Geodetic networks (HPGN). The crustal deformation measurements used in this study consist of trilateration data collected by the U.S. Geological Survey (USGS) since 1970 and Global Positioning System (GPS) location data from 1991 to 1998. We also incorporate unpublished trilateration survey data for the Mission Hills region from 1995-1997 to provide additional coverage for the Calaveras-Hayward fault stepover. Detailed station coordinates, baseline change rates, and GPS station velocities are included as a supplement to Manaker et al. (2001, submitted).

The displacement field along the Calaveras fault indicates low strain rates east of the Calaveras fault, as well as west of the Calaveras fault north of the Sunol Valley . Displacement rates indicate moderate strain rates on the block between the SAF and the Calaveras fault south of the Calaveras reservoir. This suggests that the southern and central regions of the Calaveras fault continue to pose a significant seismic hazard (Manaker, 1999, M.S. Thesis, UC Davis; Manaker et al., 2001).

We use horizontal crustal deformation rate measurements to model the three-dimensional distribution of interseismic slip rates in the seismogenic zone of the Calaveras fault. We model the horizontal surface displacement rate to be the result of horizontal strike-slip on vertical dislocations representing the Calaveras fault and the other major faults of the San Andreas system in the San Francisco Bay area. We invert for the interseismic fault slip rates using the surface displacement field and the Green's function relation for surface displacement due to dislocation in a homogeneous, isotropic, elastic half-space. We use the algorithm DIS3D to generate the Green's function matrix for the model inversion and an initial fault model developed by Bürgmann, et al. (1994) with some modifications (Manaker et al., 2001, submitted). Geological and seismological information was used to establish fault parameters (i.e., fault geometry, fault segmentation, etc.). We divide most segments into two depth ranges: a seismogenic region from 0 to ~12 km, depending on the fault; and a deep slip zone (> ~12 km) with a slip rate at the estimated long-term geologic rate. Some segments are combined to simplify the model and reflect the density of our geodetic data. Segment boundaries are based on significant changes in strike or fault behavior. We further subdivide the seismogenic range (0–12 km) of the Calaveras fault into discrete ~6 km long by 3 km deep elements (Figure 6). This discretization of the shallow and seismogenic zones provides for the estimation of the detailed slip rate distribution for comparison with the distribution of microseismicity. We also discretize segments for the Hayward and San Andreas fault that are proximal to the Calaveras fault.

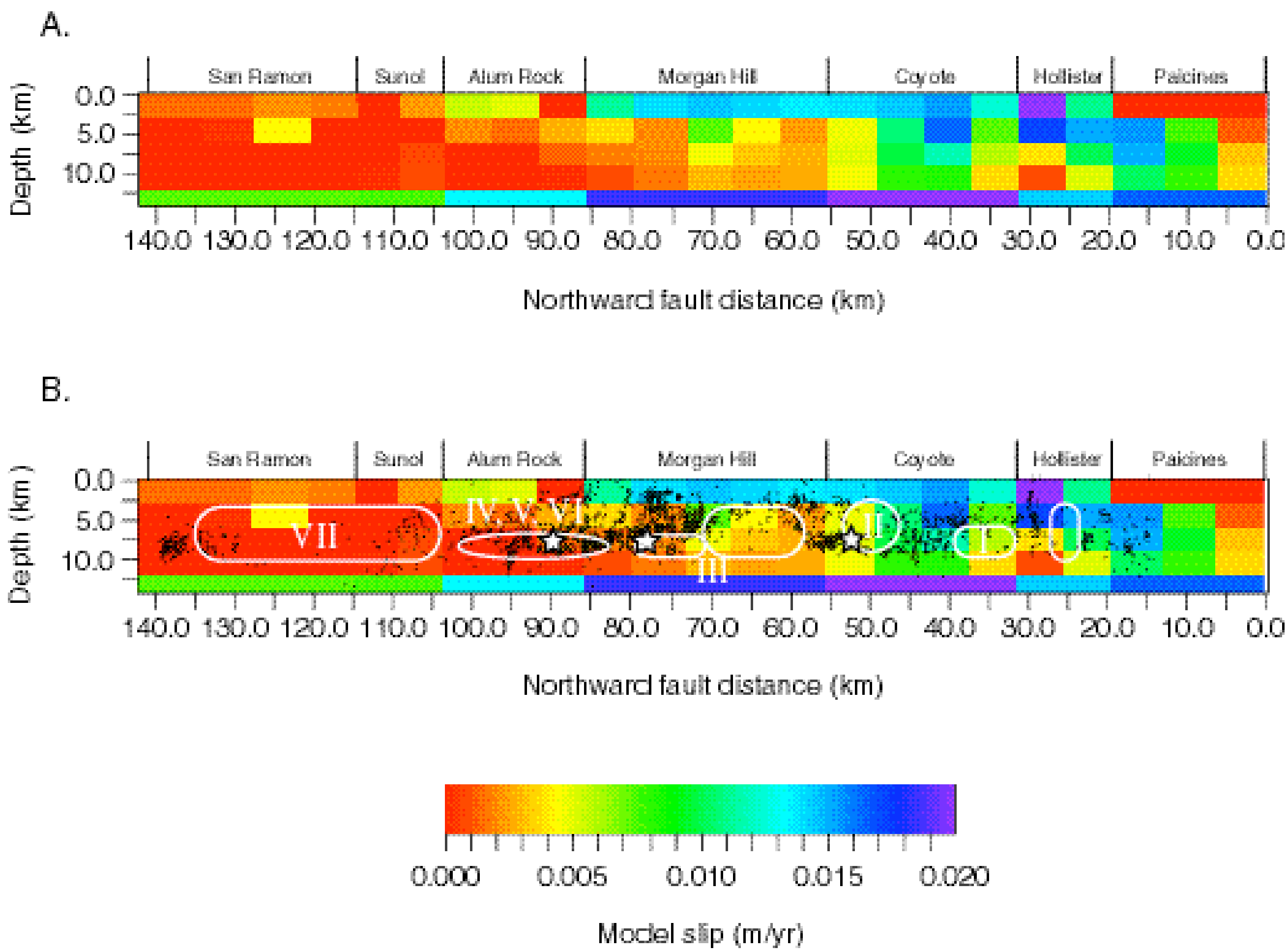

Figure 6. Modeled slip rate on the discretized Calaveras fault. The slip rates on the 6-km long x 3-km wide model elements are shown in the upper panel and compared with the distribution of microseismicity and zones of low seismicity rate identified by Oppenheimer et al. (1990) below. (from Manaker et al., 2003)

Our fault slip model consistently identifies zones of slip rate deficit that generally correspond to the locked regions suggested by Oppenheimer et al. [1990] and Oppenheimer and Lindh [1992]. The moment calculations derived from the estimated slip deficit and recurrence intervals are consistent with observed historical seismicity along the Calaveras fault. Our moment calculations based on estimated slip rate deficits suggest that these events have the potential to be of M_w 6 - 7. Events of this magnitude will likely cause significant damage to parts of the SFBR and have serious impact on the regional economy.

In general, fault slip modeling using geodetic data can be used in combination with seismicity patterns to identify specific fault regions that may be locked and accumulating strain, allowing for better characterization of seismic hazards. Continued geodetic monitoring, refinement of fault slip rate distribution models and more detailed comparisons with earthquake relocations and repeating sequences of microearthquakes similar to studies of the Hayward fault [Bürgmann et al., 2000] will provide additional information to better characterize the seismic hazard due to the Calaveras fault.

4. DATA AVAILABILITY

Data from GPS campaigns are publicly available from the UNAVCO Campaign Data Holdings Archive. Both raw GPS data and accompanying metadata are included and freely accessible at

http://archive.unavco.ucar.edu/cgi-bin/dmg/groups?cpn=1&oby=group_name

Data collected by our group for this project are archived under the Group Names of "Calaveras Fault", "Hayward Fault" and "Loma Prieta."

Please see http://www.unavco.ucar.edu/data_support/data/general.html for policies regarding the use of these freely available data. Additional data used in this study included RINEX format files obtained from the U.S. Geological Survey and the Bay Area Regional Deformation Network (BARD). These files include campaign-style surveying (USGS) and continuous GPS stations (BARD) and are available at the NCEDC at UC Berkeley.

For more information regarding data availability, contact:

Dr. Roland Bürgmann
Department of Earth and Planetary Science, University of California, Berkeley
307 McCone Hall, Berkeley, CA 994720-4767
e-mail:burgmann@seismo.berkeley.edu

URL:http://www.seismo.berkeley.edu/~burgmann

5. REFERENCES

Andrews, D. J., Oppenheimer, D. H., and Lienkaemper, J. J., 1993, The Mission Link between the Hayward and Calaveras Faults, J. Geophys. Res., v. 98, No. B7, p. 12,083-12,095.

Argus, D. F., and Gordon, R. G., 1991, Current Sierra Nevada-North America motion from very long baseline interferometry; implications for the kinematics of the western United States: Geology, v. 19, p. 1085-1088.

Aydin, A., and Page, B. M., 1984, Diverse Pliocene-Quaternary tectonics in a transform environment, San Francisco Bay region, California: Geological Society of America Bulletin, v. 95, p. 1303-1317.

Bürgmann, R., Arrowsmith, R., Dumitru, T., and McLaughlin, R., 1994b, Rise and fall of the southern Santa Cruz Mountains, California, deduced from fission track dating, geomorphic analysis, and geodetic data: J. Geophys. Res., v. 99, p. 20,181-20,202.

Bürgmann, R., Segall, P., Lisowski, M., and Svarc, J.L., 1997b, Postseismic Strain Following the 1989 Loma Prieta Earthquake From GPS and Leveling Measurements, Jour. of Geophys.Research, vol. 102, no. B3, p. 4933-4955..

Du, Y., and Aydin, A., 1993, Stress transfer during three sequential moderate earthquakes along the central Calaveras fault, California: J. Geophys. Res., v. 98, p. 9947-9962.

Ellsworth, W. L., 1990, Earthquake history, 1769-1989 in Wallace, R. E., ed., The San Andreas fault system, Calfornia, U.S. Geological Survey Professional Paper: 1515, p. 153-181.

Ferretti, A., C. Prati, and F. Rocca, Nonlinear subsidence rate estimation using pemanent scatterers in differential SAR interferometry, *IEEE Trans. Geosci. Remote Sens.*, *38*, 2202-2212, 2000.

Ferretti, A., C. Prati, and F. Rocca, Permanent scatterers in SAR interferometry, *IEEE Trans. Geosci. Remote Sens.*, *39* (1), 8-20, 2001.

Kelson, K. I., Lettis, W. R., and Lisowski, M., 1992, Distribution of geologic slip and creep along faults in the San Francisco Bay region: Calif. Div. Mines Geol. Spec. Pub., v. 113, p. 31-38.

Lienkaemper, J.J., J.S. Galehouse, and R.W. Simpson, Creep response of the Hayward fault to stress changes caused by the Loma Prieta earthquake, *Science*, *276*, 2014-2016, 1997.

Lienkaemper, J.J., D.P. Schwartz, K.I. Kelson, W.R. Lettis, G.D. Simpson, J.R. Southon, J.A. Wanket, and P.L. Williams, Timing of paleoearthquakes on the northern Hayward fault - Preliminary evidence in El Cerrito, California, *U.S. Geol. Surv. Open File Rep.*, *99-318*, 1-34, 1999.

Lienkaemper, J.J., J.S. Galehouse, and R.W. Simpson, Long-term monitoring of creep rate along the Hayward fault and evidence for a lasting creep response to 1989 Loma Prieta earthquake, *Geophys. Res. Lett.*, *28*, 2265-2268, 2001.

Lienkaemper, J. J., Borchardt, G., and Lisowski, M., 1991, Historic creeprate and potential for seismic slip along the Hayward Fault, California: J. Geophys. Res., v. 96, p. 18261-18283.

Lisowski, M., Savage, J. C., and Prescott, W. H., 1991, The velocity field along the San Andreas fault in central and southern California: J. Geophys. Res., v. 96, p. 8369-8389.

Manaker, D.M., R. Bürgmann, W.H. Prescott, and J. Langbein, Distribution of interseismic slip rates and the potential for significant earthquakes on the Calaveras fault, central California, *J. Geophys. Res.*, *doi:10.1029/2002JB001749*, 2003.

Okada, Y., Surface deformation due to shear and tensile faults in a half-space, *Bull. Seism. Soc. Am.*, *75*, 1135-1154, 1985.

Oppenheimer, D. H., Bakun, W. H., and Lindh, A. G., 1990, Slip partitioning of the Calaveras fault, California, and prospects for future earthquakes: J. Geophys. Res., v. 95, p. 8483-8498.

Oppenheimer, D. H., and Lindh, A. G., 1992. The potential for earthquake rupture of the northern Calaveras fault, *in* Borchardt, Glenn, and others, eds., Proceedings of the Second Conference on Earthquake Hazards in the Eastern San Francisco Bay Area. California Department of Conservation, Division of Mines and Geology Special Publication 113, p. 233-240.

Oppenheimer, D. H., and Macgregor-Scott, N., 1992, The seismotectonics of the eastern San Francisco Bay region: Calif. Div. Mines Geol. Spec. Pub., v. 113, p. 11-16.

Page, B. M., and Engebretson, D. C., 1984, Correlation between the geologic record and computed plate motions for central California: Tectonics, v. 3, p. 133-155.

Reasenberg, P. A., and Simpson, R. W., 1992, Response of regional seismicity to the static stress change produced by the Loma Prieta earthquake: Science, v. 255, p. 1687-1690.

Savage, J. C., and Lisowski, M., 1992, Inferred depth of creep on the Hayward fault, central California: J. Geophys. Res., v. 98, p. 787-795.

Savage, J. C., Lisowski, M., and Svarc, J. L., 1994, Postseismic deformation following the 1989 (M = 7.1) Loma Prieta, California, earthquake: J. Geophys. Res., v. 99, p. 13757-13765.

Savage, J.C., and M. Lisowski, Changes in long-term extension rates associated with the Morgan Hill and Loma Prieta earthquakes in California, Geophys. Res. Lett., 22 (7), 759-762, 1995.

Schmidt, D.A., The kinematics of faults in the San Francisco Bay area inferred from geodetic and seismic data, Ph.D. thesis, University of California, Berkeley, 2002.

Schmidt, D.A., and R. Bürgmann, Time dependent land uplift and subsidence in the Santa Clara valley, California, from a large InSAR data set, *J. Geophys. Res.*, *in press*, 2003.

Segall, P., and Harris, R., 1987, Earthquake deformation cycle on the San Andreas fault near Parkfield, California: J. Geophys. Res., v. 92, p. 10511-10525.

Thatcher, W., 1983, Nonlinear strain buildup and the earthquake cycle on the San Andreas fault: J. Geophys. Res., v. 88, p. 5893-5902.

Waldhauser, F., and W.L. Ellsworth, Fault structure and mechanics of the Hayward fault, California, from double-difference earthquake locations, *J. Geophys. Res.*, *107*, 10.1029/2000JB000084, 2002.

6. REPORTS PUBLISHED

Bürgmann, R. Schmidt, D., Nadeau, R., D'Alessio, M., Fielding, E., Lawrence, S., Manaker, D., McEvilly, T., and Murray, M.H., Earthquake potential along the northern Hayward fault, California,*Science,* 289, 1178-1182, 2000.

Bürgmann, R., P.A. Rosen, and E.J. Fielding, Synthetic aperture radar interferometry to measure Earth's surface topography and its deformation, *Annu. Rev. Earth Planet. Sci.*, *28*, 169-209, 2000.

Johnson, L.R. and R.M. Nadeau, Asperity Model of an Earthquake - Static Problem, Bull. Seismol. Soc. Amer., 92, 672-686, 2002.

Manaker, D.M., R. Bürgmann, W.H. Prescott, and J. Langbein, Distribution of interseismic slip rates and the potential for significant earthquakes on the Calaveras fault, central California, *J. Geophys. Res.*, *108* (B6), doi:10.1029/2002JB001749, 2003.

Nadeau, R.M., R.A. Uhrhammer and T.V. McEvilly, How Similar Are Repeating Earthquakes? , Seism. Res. Lett., 73, 216, 2002.

Rolandone, F., R. Bürgmann and R.M. Nadeau, Time-dependent Depth Distribution of Aftershocks: Implications for Fault Mechanics and Crustal Rheology, Seism. Res. Lett., 73, 229, 2002.

Schmidt, D.A., and R. Bürgmann, Transient tectonics of the Hayward, Calaveras, and Mission fault junction, *Eos Trans. AGU*, *82* (47), G22D-09, 2001.

Schmidt, D.A., R. Bürgmann, and S.A. Lawrence, Imaging time-dependent fault creep and basin subsidence in the San Francisco Bay Area using InSAR, *Eos Trans. AGU*, *81*, 336, 2000.

Schmidt, D.A., The kinematics of faults in the San Francisco Bay area inferred from geodetic and seismic data, Ph.D. thesis, University of California, Berkeley, 2002.

Schmidt, D.A., and R. Bürgmann, Time dependent land uplift and subsidence in the Santa Clara valley, California, from a large InSAR data set, *J. Geophys. Res.*, *submitted Oct. 2002*.

Segall, P., R. Bürgmann, and M. Matthews, Time dependent deformation following the 1989 Loma Prieta earthquake, *J. Geophys. Res.*, *105*, 5615-5634, 2000.

Templeton, D.C., R.M. Nadeau, and R. Bürgmann, Structure and kinematics at the juncture between the San Andreas and southern Calaveras faults, *Eos Trans. AGU*, *82* (47), S32E-02, 2001.